Photoaccelerated hot carrier transfer at MoS₂/WS₂: A first-principles study

Zhi-Guo Tao,[*] Guo-Jun Zhu,[*] Weibin Chu, Xin-Gao Gong, and Ji-Hui Yang [†]

Key Laboratory for Computational Physical Sciences (MOE), State Key Laboratory of Surface Physics, Department of Physics, Fudan University, Shanghai 200433, China and Shanghai Qizhi Institution, Shanghai 200232, China

Charge transfer in type-II heterostructures plays important roles in determining device performance for photovoltaic and photocatalytic applications. However, current theoretical studies of charge transfer process do not consider the effects of operating conditions such as illuminations and yield systemically larger interlayer transfer time of hot electrons in MoS₂/WS₂ compared to experimental results. Here in this work, we propose a general picture that illumination can induce interfacial dipoles in type-II heterostructures, which can accelerate hot carrier transfer by reducing the energy difference between the electronic states in separate materials and enhancing the nonadiabatic couplings. Using the first-principles calculations and the *ab initio* nonadiabatic molecular dynamics, we demonstrate this picture using MoS₂/WS₂ as a prototype. The calculated characteristic time for the interlayer transfer (60 fs) and the overall relaxation (700 fs) processes of hot electrons is in good agreement with the experiments. We further find that illumination mainly affects the ultrafast interlayer transfer process but has little effect on the relatively slow intralayer relaxation process. Therefore, the overall relaxation process of hot electrons has a saturated time with increased illumination strengths. The illumination-accelerated charge transfer is expected to universally exist in type-II heterostructures.

I. INTRODUCTION

Heterostructures with type-II band alignments, in which the conduction band minimum (CBM) and valence band maximum (VBM) reside in two separate materials, are widely used for optoelectronic applications including solar cells and photodetectors [1–4], because they can assist in the efficient separation of photoexcited electrons and holes. In type-II heterostructures, charge transfer at interfaces plays essential roles in determining device performance and therefore it is of great importance to understand the charge transfer process. However, traditional heterostructures made of three-dimensional (3D) materials usually have lattice mismatch. As a result, the interfacial structures are very complicated with defects and large system sizes, making it difficult to study the charge transfer process both experimentally and theoretically.

Thanks to the emerging of two-dimensional (2D) materials, van der Waals (vdW) heterostructures made of different 2D materials with clean interfaces provide a simple platform for studying the charge transfer process as well as exploring devices such as ultrathin photodetectors [5,6], tunneling transistors [7–9], and solar cells [10,11]. Contrary to our conventional wisdom, although the layer coupling is weak in vdW type-II heterostructures, ultrafast interlayer charge transfers [12–15] are observed. Wang *et al.* [12] experimentally reported that hot holes transfer from the MoS₂ layer to the WS₂ layer within 50 femtoseconds (fs). Chen *et al.* [13] observed that hot electrons transfer from the WS₂ layer to the MoS₂ layer within 50 fs and then relax to the band edge after about 800 fs. Theoretically, Zhang *et al.* [16] used time-dependent density functional theory (TDDFT) to simulate the ultrafast transfer of holes and they reported a time scale of 100 fs. Zheng *et al.* [17] used *ab initio* nonadiabatic molecular dynamics (NAMD) to simulate the relaxation of electrons and they found that about 3/4 of the electrons relax to the band edge after 1000 fs. We find that theoretically simulated charge transfer time is systematically longer than the experimental results. Although there could be many reasons for the discrepancy between experiments and theories such as substrates, interfacial defects, inaccurate DFT band structures of ground states, etc., one fact that photoinduced electrons and holes will definitely affect the electronic band structures at the interface is not considered in previous theoretical works. Consequently, whether and how illumination plays roles in the process of interfacial charge transfer is not known, revealing which is not only important for understanding light-matter interaction but also will benefit optoelectronic performance of many 2D and 3D devices.

In this paper, we investigate the effect of illumination on the ultrafast transfer and relaxation of hot electrons at type-II heterostructures. We propose a general picture that the photoinduced electrons and holes residing in different materials of type-II heterostructures will form an interfacial dipole, which reduces band energy difference in separate materials, thus accelerating hot electron transfer. We demonstrate our picture in the WS₂/MoS₂ heterostructure. Using the first-principles calculation methods and NAMD simulation techniques, we systematically explore the dynamics of hot electrons under

---

[*]These authors contributed equally to this work.
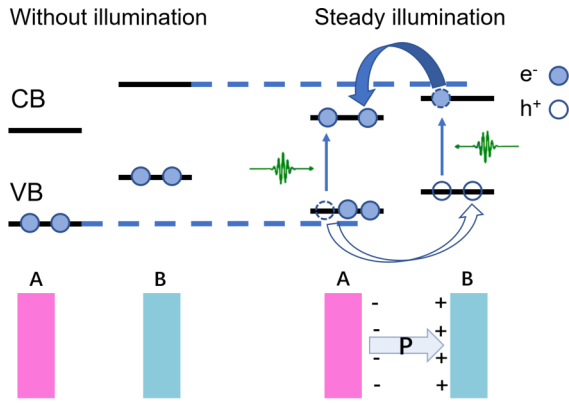
[†]jhyang04@fudan.edu.cn

FIG. 1. A schematic diagram to show the photoexcitation and carrier transfer in an *A/B* heterostructure with/without illumination. The dashed circle represents carriers transferring from *A*(*B*) to *B*(*A*).

FIG. 2. Band structure of the MoS_2/WS_2 heterostructure and the electronic characters of considered states. The Brillion zone is shown in the inset. The color map indicates the orbital contributions from different materials, i.e., red for WS_2 and blue for MoS_2.

different illumination strengths. Our simulation results indicate that the transfer of hot electrons is indeed accelerated under illumination and the calculated transfer time is in excellent agreement with experimental results [13]. We expect that illumination-accelerated charge transfer is universal in both 2D and 3D type-II heterostructures.

II. COMPUTATIONAL DETAILS

The density functional theory (DFT) calculations are performed using the Vienna *ab initio* simulation package (VASP) [18–20]. The electron and core interactions are treated using the frozen-core projected augmented wave (PAW) approach [21]. For all the calculations, the generalized gradient approximation (GGA) formulated by Perdew, Burke, and Ernzerhof (PBE) [22] is adopted. The van der Waals (vdW) interactions are considered using the DFT-D2 [23] method. To simulate the steady illumination conditions, the constrained occupation method [24,25] is used, in which fractional electrons are removed from the VBM to the CBM of the whole heterostructure. For the calculations of electronic structures, an energy cutoff of 400 eV and an $18 \times 18 \times 1$ *k*-point mesh are adopted. To study the charge transfer process, we perform the nonadiabatic molecular dynamic simulations (NAMD) as implemented in the Hefei-NAMD code [26]. Hefei-NAMD implemented within time domain density functional theory (TD-DFT) in the Kohn-Sham (KS) framework, which augments the Vienna *ab initio* simulation package (VASP) with employing the Fewest Switches Surface Hopping (FSSH) technique [27,28] and classical path approximation [29]. The Γ point is used in the *ab initio* molecular dynamic (AIMD) simulations for an orthogonal $3 \times 3 \times 1$ supercell of MoS_2/WS_2 with 108 atoms. We sample 1×10^4 trajectories for 1 ps with a time step of 1 fs. The NAMD results are based on averaging over 100 different initial configurations. The nonadiabatic couplings are calculated using CANAC with phase correction and state tracking [30–33].

III. RESULT AND DISCUSSION

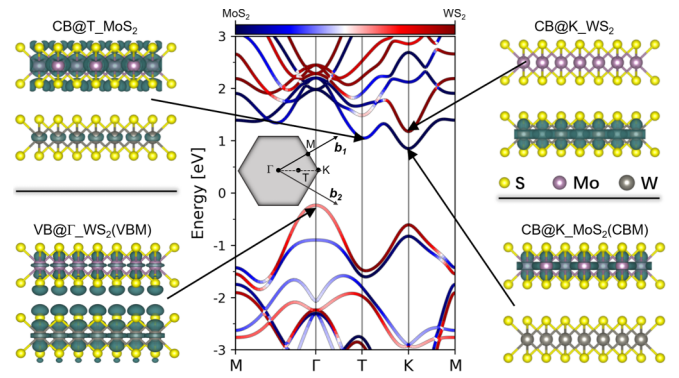The band diagram of a typical type-II heterostructure is shown in Fig. 1. Before illumination, the CBM and VBM of

material *B* are higher than the CBM and VBM of material *A*, respectively. The band offsets are ΔE_c and ΔE_v for the CBM and VBM, respectively. Under illumination, electrons are excited from the valance band to the conduction band in either *A* or *B* or both, depending on the photon energies and band gaps. Driven by thermodynamic effects, the excited carriers will finally relax to the band edges of the whole heterostructure, i.e., electrons will relax to the CBM of *A* and holes will relax to the VBM of *B*. Consequently, an interfacial dipole will form, which will push the bands in *A* upwards and pull the bands in *B* downwards, respectively, thus reducing the energy differences between bands in *A* and bands in *B*, i.e., ΔE_c and ΔE_v will be reduced. In this case, if there is a hot electron in *B*, it will be easier for it to transfer to *A* and interlayer charge transfer will be accelerated. Such a picture is expected to commonly exist in type-II heterostructures.

To demonstrate the above picture and quantitatively determine the effects of photoinduced interfacial dipoles on charge transfer at type-II heterostructures, we theoretically study the charge transfer at MoS_2/WS_2 considering the illumination conditions using NAMD. Before presenting the simulation results, we first discuss the band structure of the MoS_2/WS_2 heterostructure. Here we consider the $C7$ stacking of MoS_2 and WS_2 as it is previously reported to be the most stable [34,35]. In MoS_2 or WS_2 monolayer, both the VBM and CBM states lie at the *K* point. When they are stacked, the band edges at the *K* point are distributed in separate materials. As seen in Fig. 2, the lowest conduction band edge at the *K* point mainly resides in MoS_2 (denoted as CB@K_MoS_2) while the higher conduction band edge at the *K* point mainly resides in WS_2 (denoted as CB@K_WS_2). Similarly, the higher (lower) valence band edge at the *K* point mainly resides in WS_2 (MoS_2). Such kinds of band edge distributions clearly indicates that the system is a type-II heterostructure. We note that the overall VBM of the heterostructure lies at the Γ point, compared to the VBM in MoS_2 or WS_2 monolayer being located at the *K* point. The difference mainly results from the interlayer orbital hybridization due to interlayer interactions, as we find that the VBM is distributed in both MoS_2 and WS_2 (see Fig. 2). Because this state resides more in WS_2, we denote

it as VB@Γ_WS$_2$. Our calculated band structure agrees well with previous studies [17,36].

Upon illumination by low-energy photons which have energies slightly larger than the band gaps of MoS$_2$ or WS$_2$, electrons will be excited from the valence band edges to the conduction band edges in MoS$_2$ and/or in WS$_2$. Then the hot electrons (holes) will relax and transfer to the CB@K_MoS$_2$ (VB@Γ_WS$_2$) finally. Here we mainly focus on the transfer and relaxation of hot electrons from the CB@K_WS$_2$ to the CB@K_MoS$_2$. Note that between the CB@K_WS$_2$ and CB@K_MoS$_2$, there is an intermediate state which is located at the T valley. Electronic character analysis shows that this state is mainly contributed by the electronic state of MoS$_2$ with a small part distributed in WS$_2$, indicating that it is a hybridized state. Nevertheless, we still denote this state as CB@T_MoS$_2$. Previous studies [17] show that such as intermediate state can help the electron transfer and relaxation following the route of CB@K_WS$_2$–>CB@T_MoS$_2$–>CB@K_MoS$_2$ while it is difficult for hot electrons to directly transfer from CB@K_MoS$_2$ to CB@K_WS$_2$. Their results show that it takes more than 1000 fs for hot electrons to relax from CB@K_WS$_2$ to CB@K_MS$_2$, which is longer than the experimental results (800 fs), as no illumination conditions are considered.

Once illumination is applied, hot carrier transfer and relaxation happens. Since the overall CBM and VBM of the heterostructure are distributed in different layers, holes will be enriched in WS$_2$ while electrons will be enriched in MoS$_2$. Therefore, we can simulate the illumination conditions by constraining the electron occupations at different states. At room temperature, the experimentally observed the photoexcited carrier densities [12,13] in the MoS$_2$/WS$_2$ heterostructure are about 10^{12}–10^{13} cm^{-2}, which corresponds to exciting about 0.1 electrons from the VB@Γ_WS$_2$ (VBM) to the CB@K_MoS$_2$ (CBM) in our simulated $3 \times 3 \times 1$ supercell. To mimic the illumination effects on hot electron transfer under experimental operation conditions and make direct comparisons, the light intensity of our simulation should be equivalent to the experimental. In addition, we need to verify that our results are consistent with the previous simulations without illumination. Consequently, here we consider three illumination conditions ($\alpha = 0, 0.05, 0.1$), which correspond to the photoexcited carrier densities of 0, 3.16×10^{12}, and 6.32×10^{12} cm^{-2}, respectively.

Now we consider the hot electron transfer and relaxation under different illumination conditions. As mentioned above, the total relaxation path of hot electrons, that is, CB@K_WS$_2$–>CB@T_MoS$_2$–>CB@K_MoS$_2$, can be divided into two processes: hot electron transfer between layers (CB@K_WS$_2$–>CB@T_MoS$_2$) and electron relaxation in MoS$_2$ (CB@T_MoS$_2$–>CB@K_MoS$_2$) after transfer. Using the NAMD simulations, we can obtain the transfer and total relaxation time of hot electrons. Our results are shown in Fig. 3. Initially, one hot electron is put at the CB@K_WS$_2$ state. If more than 0.5 electrons evolve to another state with time, then we say the transfer or the relaxation occurs. Without illumination, our results show that it takes near 270 fs for the hot electron to transfer from the CB@K_WS$_2$ to the CB@T_MoS$_2$ and the total relaxation time from the CB@K_WS$_2$ to the CB@K_MoS$_2$ state is about 1000 fs [see
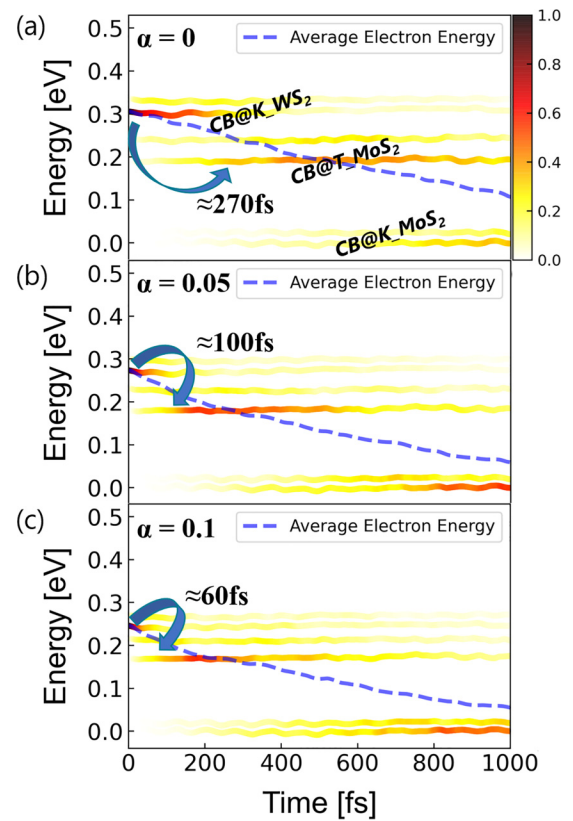

FIG. 3. Simulation results for the evolution of a hot electron from the CB@K_WS$_2$ state to the CB@K_MoS$_2$ state. (a)–(c) Time evolutions of the electron occupations and averaged electron energy at 300 K under different illumination strengths. The colorful strips indicate the electron occupations of relevant energy states as time evolves, and the dashed line represents the averaged electron energy. The energy reference is the averaged CBM energy.

Fig. 3(a)]. While our results are similar to previous theoretical studies [17], the time values are larger than the experimental measurements [13]. When the illumination strength corresponds to the photoexcitation of 0.05 electrons between the overall band edges of the heterostructure, the transfer and overall relaxation time of the hot electron are 100 and 700 fs, respectively [see Fig. 3(b)]. As the illumination strength further increases corresponding to the photoexcitation of 0.1 electrons, the transfer time of hot electrons further reduces to about 60 fs while the overall relaxation time is barely reduced further. We note that these two characteristic time values under illumination conditions are in good agreement with the experiment [13]. The discrepancies between previous theoretical results and experimental values are thus due to the illumination conditions in our opinions.

We further simulate the interlayer charge transfer process CB@K_WS$_2$–>CB@T_MoS$_2$ and the intralayer charge relaxation process CB@T_MoS$_2$–>CB@K_MoS$_2$ separately to obtain more understanding about the illumination effects on hot electron behaviors at the heterostructure. As shown in Fig. S1 of the Supplemental Material [37], our results show that illumination can accelerate the interlayer transfer of hot electrons but has negligible effects on the intralayer relaxation with the time scale of the second process much longer than
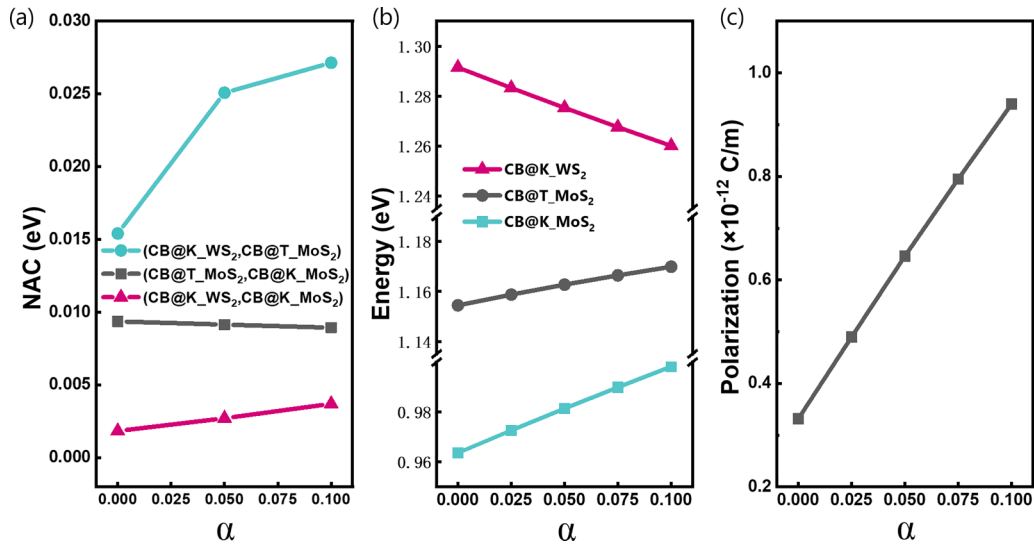
FIG. 4. Interfacial carrier-dynamics-related properties dependence on illumination strengths. (a) The averaged absolute values of the NAC between considered electronic states under different illumination strengths. (b),(c) The energy levels and interfacial dipole dependence on illumination strengths, respectively.

that of the first one. Consequently, the main bottleneck of the overall hot electron relaxation process is actually the intralayer relaxation. This explains why the overall relaxation of the hot electron tends to saturate with increased illumination strengths.

To understand why illumination accelerates the interlayer transfer of the hot electron, we turn to analyze the carrier dynamics between different energy states determined by the nonadiabatic coupling (NAC) term [38–44], which is given by

$$d_{ij} = \left\langle \varphi_i \left| \frac{\partial}{\partial t} \right| \varphi_j \right\rangle = \frac{\langle \varphi_i | \nabla_R H | \varphi_j \rangle}{\epsilon_j - \epsilon_i} \dot{R},$$

where H is the Kohn-Sham Hamiltonian, φ_i, φ_j, ϵ_i, and ϵ_j are the wave functions and eigenvalues for the electronic states j and k, respectively, and $\dot{R}$ is the velocities of nuclei. Note that, the probability of electron transition is proportional to the square of NAC and larger NAC indicates faster electron transitions between two electronic states. Our results in Fig. 4(a) show that the averaged NAC between the CB@K_WS$_2$ and CB@K_MoS$_2$ states is small compared to the one between the CB@K_WS$_2$ and CB@T_MoS$_2$ states as well as the one between the CB@T_MoS$_2$ and CB@K_MoS$_2$ states, suggesting that the direct electron transitions from the CB@K_WS$_2$ to the CB@K_MoS$_2$ is very difficult while the combined interlayer transfer and intralayer relaxation, i.e., CB@K_WS$_2$–>CB@T_MoS$_2$–>CB@K_MoS$_2$, is the dominant mechanism for the electron relaxation at the heterostructure. Our analysis is consistent with previous works [17].

Now we see how illumination affects the NAC terms. As shown in Fig. 4(a), the averaged NAC between the CB@K_WS$_2$ and CB@T_MoS$_2$ states increases with the increase of light intensity. In contrast, the NAC between the CB@T_MoS$_2$ and CB@K_MoS$_2$ states is little affected by the illumination. The changes of the NAC terms under the illumination conditions thus explain the accelerated interlayer

charge transfer as well as the nearly unaffected intralayer charge relaxation.

To understand the underlying mechanism behind the illumination effects on the NAC terms, we note that the NAC value is inversely proportional to the energy difference between the two states and is proportional to the atomic velocities as well as the electron-phonon couplings. The electron-phonon couplings can be reflected by the energy fluctuations of the Kohn-Sham states in the molecular dynamical simulation [see Figs. S2(a)–S2(c) [37]] or more clearly by the corresponding Fourier transform (FT) spectra [39,40] [see Figs. S2(d)–S2(f) [37]]. As we can see, the amplitudes of the three conduction band energy fluctuations are basically the same under different illumination conditions, indicating that the electron-phonon coupling strength is little affected by illuminations. This is understandable because in our simulation process, the temperature of the system is maintained as 300 K and therefore the illumination effect on atomic vibrations should be negligible if no heating effect is considered. Similarly, the velocities of nuclei are also expected to have little change. Consequently, illumination affects the NAC terms mainly through affecting the band energy differences. Indeed, from Figs. S2(a)–S2(c) [37], we can see that there are clear changes of the energy differences between MoS$_2$ and WS$_2$ bands with varying illumination strengths.

To study how the energy level changes with illumination strengths, we calculate the electronic structures of the heterostructure under the illumination conditions using the equilibrium structure. As shown in Fig. 4(b), with the illumination strengths increasing, the energy levels of the CB@T_MoS$_2$ and CB@K_MoS$_2$ states are increased, while the energy level of the CB@K_WS$_2$ state is decreased. According to Fig. 1, we know that under the illumination conditions, electrons are enriched in MoS$_2$ and holes are enriched in WS$_2$, inducing the dipole across the heterostructure. The stronger the illumination strength, the larger the dipole [as shown in Fig. 4(c)], which reduces the electrostatic potential

in MoS_2 and increases that in WS_2, leading to the increase of the energy level of the MoS_2 layer and the decrease of the energy level of the WS_2 layer. Accordingly, the energy level difference between the CB@K_WS_2 and CB@T_MoS_2 changes from 137 meV when there is no illumination to 90 meV when the illumination strength is 0.1 [see Fig. 4(b)], which is reduced by as much as 1/3. Consequently, the NAC term increases, leading to the accelerated interlayer electron transfer. In contrast, the energy difference between the CB@T_MoS_2 and CB@K_MoS_2 is only slightly reduced because the CB@T_MoS_2 is a hybrid state with a small part of it distributed in WS_2. In addition, with the increased illumination, the distribution of CB@T_MoS_2 orbit in the WS_2 layer is slightly increased (see Table S1 of the Supplemental Material [37]), which might weaken the coupling between CB@T_MoS_2 and CB@K_MoS_2. The consequence is that the NAC term between the CB@T_MoS_2 and CB@K_MoS_2 is nearly unchanged under illumination and therefore the intralayer electron relaxation is little affected. Note that, although the energy level difference between the CB@K_WS_2 and CB@K_MoS_2 has a large decrease under illumination, the relatively large energy difference always leads to the very small NAC term whether the system is under illumination or not. Consequently, the direct electron transition from the CB@K_WS_2 to the CB@K_MoS_2 can be reasonably ignored.

Here we have used the simple MoS_2/WS_2 system as an example to demonstrate the general effects of the illumination on the charge transfer at a type-II heterostructure. Note that the ultrafast transfer of hot electrons from the WS_2 layer to the MoS_2 layer via the CB@T_MoS_2 energy level indicates that a hybridized intermediate state, which is located in between the band edge states of two materials in a type-II heterostructure, can accelerate carrier transfer and enhance carrier separations, especially under illumination conditions. Consequently, the performance of optoelectronic devices might be improved through creating such intermediate states, i.e., by inserting some window layer in type-II heterostructures. Another thing we want to point out is that, although the interfacial dipole enhances the electron transfer by reducing band energy differences in separated layers, electrons in MoS_2 must be extrapolated in time. Otherwise, accumulated electrons in MoS_2 will increase the dipole field, thus preventing interfacial electron transfer. Under very strong illuminations, i.e., in concentrated solar cells, once the extrapolation speed is surpassed by the transfer speed, the device efficiencies might be reduced [45,46]. Therefore, by manipulating illumination strengths to make the charge transfer and carrier extrapolation processes coordinate, device performance could be enhanced.

IV. CONCLUSION

In summary, we have investigated the effect of illumination on the ultrafast transfer and relaxation of hot electrons in the MoS_2/WS_2 heterostructure. We have demonstrated the picture that the interfacial dipole induced by illumination can reduce the energy difference between the states in MoS_2 and those in WS_2, thus accelerating interlayer transfer of hot electrons by enhancing the nonadiabatic couplings. We expect that this picture can be widely applied to understand the carrier transfer in both 2D and 3D type-II heterostructures. In additions, based on our studies, we propose that it might offer a feasible strategy to improve the performance of optoelectronic devices by manipulating illumination strengths to have coordinate charge transfer and carrier extrapolation processes.

[1] C. Deibel, T. Strobel, and V. Dyakonov, Role of the charge transfer state in organic donor–acceptor solar cells, Adv. Mater. **22**, 4097 (2010).

[2] A. J. Heeger, 25th anniversary article: Bulk heterojunction solar cells: Understanding the mechanism of operation, Adv. Mater. **26**, 10 (2014).

[3] H. Zhou, Q. Chen, G. Li, S. Luo, T. Song, H. Duan, Z. Hong, J. You, Y. Liu, and Y. Yang, Interface engineering of highly efficient perovskite solar cells, Science **345**, 542 (2014).

[4] M. A. Green, A. Ho-Baillie, and H. J. Snaith, The emergence of perovskite solar cells, Nat. Photonics **8**, 506 (2014).

[5] L. Britnell, R. M. Ribeiro, A. Eckmann, R. Jalil, B. D. Belle, A. Mishchenko, Y. Kim, R. V. Gorbachev, T. Georgiou, and S. V. Morozov, Strong light-matter interactions in heterostructures of atomically thin films, Science **340**, 1311 (2013).

[6] W. J. Yu, Y. Liu, H. Zhou, A. Yin, Z. Li, Y. Huang, and X. Duan, Highly efficient gate-tunable photocurrent generation in vertical heterostructures of layered materials, Nat. Nanotechnol. **8**, 952 (2013).

[7] L. Britnell, R. V. Gorbachev, R. Jalil, B. D. Belle, F. Schedin, A. Mishchenko, T. Georgiou, M. I. Katsnelson, L. Eaves, and S. V. Morozov, Field-effect tunneling transistor based on vertical graphene heterostructures, Science **335**, 947 (2012).

[8] T. Georgiou, R. Jalil, B. D. Belle, L. Britnell, R. V. Gorbachev, S. V. Morozov, Y. Kim, A. Gholinia, S. J. Haigh, and O. Makarovsky, Vertical field-effect transistor based on graphene-WS_2 heterostructures for flexible and transparent electronics, Nat. Nanotechnol. **8**, 100 (2013).

[9] K. Roy, M. Padmanabhan, S. Goswami, T. P. Sai, G. Ramalingam, S. Raghavan, and A. Ghosh, Graphene-MoS_2 hybrid structures for multifunctional photoresponsive memory devices, Nat. Nanotechnol. **8**, 826 (2013).

[10] X. Li, W. Chen, S. Zhang, Z. Wu, P. Wang, Z. Xu, H. Chen, W. Yin, H. Zhong, and S. Lin, 18.5% efficient graphene/GaAs van der Waals heterostructure solar cell, Nano Energy **16**, 310 (2015).

[11] A. Rawat, R. Ahammed, N. Jena Dimple, M. K. Mohanta, and A. De Sarkar, Solar energy harvesting in type II van der Waals

heterostructures of semiconducting group III monochalcogenide monolayers, J. Phys. Chem. C **123**, 12666 (2019).

[12] X. Hong, J. Kim, S. Shi, Y. Zhang, C. Jin, Y. Sun, S. Tongay, J. Wu, Y. Zhang, and F. Wang, Ultrafast charge transfer in atomically thin MoS$_2$/WS$_2$ heterostructures, Nat. Nanotechnol. **9**, 682 (2014).

[13] H. Chen, X. Wen, J. Zhang, T. Wu, Y. Gong, X. Zhang, J. Yuan, C. Yi, J. Lou, P. M. Ajayan, W. Zhuang, G. Zhang, and J. Zheng, Ultrafast formation of interlayer hot excitons in atomically thin MoS$_2$/WS$_2$ heterostructures, Nat. Commun. **7**, 12512 (2016).

[14] Z. Ji, H. Hong, J. Zhang, Q. Zhang, W. Huang, T. Cao, R. Qiao, C. Liu, J. Liang, and C. Jin, Robust stacking-independent ultrafast charge transfer in MoS$_2$/WS$_2$ bilayers, ACS Nano **11**, 12020 (2017).

[15] C. Jin, E. Y. Ma, O. Karni, E. C. Regan, F. Wang, and T. F. Heinz, Ultrafast dynamics in van der Waals heterostructures, Nat. Nanotechnol. **13**, 994 (2018).

[16] H. Wang, J. Bang, Y. Sun, L. Liang, D. West, V. Meunier, and S. Zhang, The role of collective motion in the ultrafast charge transfer in van der Waals heterostructures, Nat. Commun. **7**, 11504 (2016).

[17] Y. Tian, Q. Zheng, and J. Zhao, Tensile strain-controlled photogenerated carrier dynamics at the van der Waals heterostructure interface, J. Phys. Chem. Lett. **11**, 586 (2020).

[18] G. Kresse and J. Hafner, Ab initio molecular dynamics for open-shell transition metals, Phys. Rev. B **48**, 13115 (1993).

[19] G. Kresse and J. Furthmüller, Efficient iterative schemes for ab initio total-energy calculations using a plane-wave basis set, Phys. Rev. B **54**, 11169 (1996).

[20] G. Kresse and J. Furthmüller, Efficiency of ab-initio total energy calculations for metals and semiconductors using a plane-wave basis set, Comput. Mater. Sci. **6**, 15 (1996).

[21] P. E. Blöchl, Projector augmented-wave method, Phys. Rev. B **50**, 17953 (1994).

[22] J. P. Perdew, K. Burke, and M. Ernzerhof, Generalized Gradient Approximation Made Simple, Phys. Rev. Lett. **77**, 3865 (1996).

[23] S. Grimme, Semiempirical GGA-type density functional constructed with a long-range dispersion correction, J. Comput. Chem. **27**, 1787 (2006).

[24] P. Ramos and M. Pavanello, Low-lying excited states by constrained DFT, J. Chem. Phys. **148**, 144103 (2018).

[25] T. Kowalczyk, S. R. Yost, and T. V. Voorhis, Assessment of the ΔSCF density functional theory approach for electronic excitations in organic dyes, J. Chem. Phys. **134**, 054128 (2011).

[26] Q. Zheng, W. Chu, C. Zhao, L. Zhang, H. Guo, Y. Wang, X. Jiang, and J. Zhao, Ab initio nonadiabatic molecular dynamics investigations on the excited carriers in condensed matter systems, Wires Comput. Mol. Sci. **9**, e1411 (2019).

[27] J. C. Tully, Molecular dynamics with electronic transitions, J. Chem. Phys. **93**, 1061 (1990).

[28] J. R. Schmidt, P. V. Parandekar, and J. C. Tully, Mixed quantum-classical equilibrium: Surface hopping, J. Chem. Phys. **129**, 044104 (2008).

[29] A. V. Akimov and O. V. Prezhdo, The PYXAID program for non-adiabatic molecular dynamics in condensed matter systems, J. Chem. Theory Comput. **9**, 4959 (2013).

[30] S. Fernandez-Alberti, A. E. Roitberg, T. Nelson, and S. Tretiak, Identification of unavoided crossings in nonadiabatic photoexcited dynamics involving multiple electronic states in polyatomic conjugated molecules, J. Chem. Phys. **137**, 14512 (2012).

[31] A. V. Akimov, A simple phase correction makes a big difference in nonadiabatic molecular dynamics, J. Phys. Chem. Lett. **9**, 6096 (2018).

[32] W. Chu and O. V. Prezhdo, Concentric approximation for fast and accurate numerical evaluation of nonadiabatic coupling with projector augmented-wave pseudopotentials, J. Phys. Chem. Lett. **12**, 3082 (2021).

[33] W. Chu, Q. Zheng, A. V. Akimov, J. Zhao, W. A. Saidi, and O. V. Prezhdo, Accurate computation of nonadiabatic coupling with projector augmented-wave pseudopotentials, J. Phys. Chem. Lett. **11**, 10073 (2020).

[34] K. Kośmider and J. Fernández-Rossier, Electronic properties of the MoS$_2$-WS$_2$ heterojunction, Phys. Rev. B **87**, 075451 (2013).

[35] Y. Gong, J. Lin, X. Wang, G. Shi, S. Lei, Z. Lin, X. Zou, G. Ye, R. Vajtai, and B. I. Yakobson, Vertical and in-plane heterostructures from WS$_2$/MoS$_2$ monolayers, Nat. Mater. **13**, 1135 (2014).

[36] Q. Zheng, W. A. Saidi, Y. Xie, Z. Lan, O. V. Prezhdo, H. Petek, and J. Zhao, Phonon-assisted ultrafast charge transfer at van der Waals heterostructure interface, Nano Lett. **17**, 6435 (2017).

[37] See Supplemental Material at http://link.aps.org/supplemental/10.1103/PhysRevB.108.014312 for simulation results for the interlayer charge transfer and the intralayer charge relaxation process under different illumination strengths, time evolutions of the Kohn-Sham states in the molecular dynamical simulation and the corresponding Fourier transform spectra, the dependence of the electronic character of the CB@T_MoS2 state on the illumination strengths, and the convergence test of cutoff energy.

[38] W. R. Duncan, W. M. Stier, and O. V. Prezhdo, Ab initio nonadiabatic molecular dynamics of the ultrafast electron injection across the alizarin-TiO$_2$ interface, J. Am. Chem. Soc. **127**, 7941 (2005).

[39] H. Guo, W. Chu, Q. Zheng, and J. Zhao, Tuning the carrier lifetime in black phosphorene through family atom doping, J. Phys. Chem. Lett. **11**, 4662 (2020).

[40] L. Zhang, Q. Zheng, Y. Xie, Z. Lan, O. V. Prezhdo, W. A. Saidi, and J. Zhao, Delocalized impurity phonon induced electron-hole recombination in doped semiconductors, Nano Lett. **18**, 1592 (2018).

[41] Q. Zheng, Y. Xie, Z. Lan, O. V. Prezhdo, W. A. Saidi, and J. Zhao, Phonon-coupled ultrafast interlayer charge oscillation at van der Waals heterostructure interfaces, Phys. Rev. B **97**, 205417 (2018).

[42] C. Zhao, Q. Zheng, J. Wu, and J. Zhao, Ab initio nonadiabatic molecular dynamics investigation on the dynamics of photogenerated spin hole current in Cu-doped MoS$_2$, Phys. Rev. B **96**, 134308 (2017).

[43] Y. Wang, Y. Shi, C. Zhao, Q. Zheng, and J. Zhao, Photogenerated carrier dynamics at the anatase/rutile TiO$_2$ interface, Phys. Rev. B **99**, 165309 (2019).

[44] W. Chu, W. A. Saidi, Q. Zheng, Y. Xie, Z. Lan, O. V. Prezhdo, H. Petek, and J. Zhao, Ultrafast dynamics of photongenerated holes at a CH$_3$OH/TiO$_2$ rutile interface, J. Am. Chem. Soc. **138**, 13740 (2016).

[45] T. Harada, N. Miyashita, T. Ikari, and A. Fukuyama, Effect of concentrated sunlight illumination on mobility and concentrator solar cell efficiency, Jpn. J. Appl. Phys. **59**, 071002 (2020).

[46] G. Li, Y. Lu, Q. Xuan, Y. G. Akhlaghi, G. Pei, J. Ji, and X. Zhao, Small scale optimization in crystalline silicon solar cell on efficiency enhancement of low-concentrating photovoltaic cell, Sol. Energy **202**, 316 (2020).